Comparison of physical property–porosity behaviour with minimum solid area models

R. W. RICE
Consultant, 5411 Hopark Dr., Alexandria, VA 22310–1109

An extensive survey of the porosity dependence of (room temperature) physical properties shows that mechanical properties and electrical and thermal conductivity, i.e. properties dependent on the local flux or fields in the material, follow minimum solid area models. This is shown extensively for elastic properties and tensile (flexure) strength, but consistency with other properties, e.g. compressive strength, hardness, electrical and thermal conductivity is also shown. Although data for ceramics is most extensive, data for rocks, metals, and carbon are included, since the consistency of these, especially of metals with ceramics, provides important support for the minimum solid area concept. While porosity characterization is generally minimal, expected model trends with pore character are corroborated by correlating processing and resultant expected pore character with porosity–property results. It is argued that properties dependent on mass should be better fit by a linear, i.e. rule of mixture, relationship between such properties and porosity. Support for this is shown in dielectric constant–porosity data.

1. Introduction

Despite extensive study, much remains to be understood about the porosity dependence of physical properties of ceramics and other materials. In particular, until recently, there has not been a predictive capability, [1] i.e., the ability to even approximately determine what the porosity dependence of properties would be given only the amount and character of the porosity. Several studies [2–11], including some quite recent ones, have examined the applicability of various models to ceramic mechanical property–porosity data. Such studies, which focused on the closeness of fit between various equations and the available data, are useful for indicating models that often provide very poor fit to data and hence are suspect or inappropriate. Although some models contain fewer and some more parameters (e.g. models 1–4 and 5–7, respectively; Table I), with the latter, in principle, providing more opportunity for effective curve fitting, this is not always so in practice. Equations for some given models have often been generalized by letting constants in the resulting equations which are defined by the assumed pore geometry be parameters in curve fitting. However, this has not significantly aided predictability, i.e. relating the equation parameters to the amount and character of the porosity. Lacking such a definitive porosity–property relationship, one can always seek more effective empirical curve fitting, but this has been unsuccessful in effectively differentiating between various models for two basic reasons.

The first reason that many of these previous curve fitting studies have not been successful in truly discriminating between the different models that fit porosity data, at least approximately, is that the data are often variable in quality. For example, the comparative studies of Dean and Lopez [2] show that ThO_2 and MgO data were significant factors in discriminating between models in their analysis. However, the investigators who generated the ThO_2 data noted it was variable due to heterogeneous porosity [12]. Different MgO data sets showed substantial variation in the porosity dependence of Poisson's ratio (v), varying from increasing, approximately independent of, or decreasing with increasing porosity [13]. Besides showing considerable data variation, this probably indicates the effects of inhomogeneous porosity since there is no theoretical basis for v increasing with increasing levels of uniformly distributed porosity [14]. However, this could result from heterogeneously distributed porosity effecting measurements to determine v. Although not commonly checked for, inhomogeneous distribution of porosity is probably fairly common, and a serious problem, as discussed later.

The second and most fundamental reason why these previous curve fitting studies have been limited in their effectiveness of identifying truly predictive models has been that previous, potentially predictive models have been based on a single, fixed character of porosity (e.g. all bubbles, or all pores between particles of fixed shapes and stackings). In reality, both mixtures and changes of porosity need to be considered. Most porous bodies, as formed, contain more than one type of porosity [1], e.g. partially sintered bodies of various particle sizes and packings result in varying porosity character. Since such variations are built into

TABLE I Fit of various property–porosity equations[a]

Property[b]	Method of comparison[c]	1 $1 - bP$	2 e^{-bP}	3 $\dfrac{1-P}{1+bP}$	4 $1 - bP^{2/3}$	5 $(1-bP)^m$	6 $1 - b_1 P + b_2 P^2$	7 $e^{(-b_1 P - b_2 P^2)}$	Material	Investigator
E	coefficient of variation	2.9	6.0	5.0	2.7				16 sets of data for 11 oxides	
G	"	2.0	4.2	4.1	2.7				11 sets of data for 8 oxides	Dean and Lopez [2]
E	% error	1.9	1.4	2.2					Dy_2O_3	Manning et al. [3]
		2.2	2.3	2.4					Er_2O_3	
		1.9	1.9	2.0					Ho_2O_3	
		1.2	2.0	2.2					Y_2O_3	
G	"	1.8	1.5	1.6					Dy_2O_3	Manning et al. [3]
		1.9	2.1	2.1					Er_2O_3	
		1.8	2.0	2.4					Ho_2O_3	
		1.6	2.0	2.1					Y_2O_3	
E	rank	2	3	4			1		Al_2O_3	De Portu and Vincenzini [4]
E	standard error	17.9	26.6	7100		12.2		13.7	Al_2O_3	Phani and Niyogi [5]
E	"	21.3	15.2	14.8		11.8		10.9		
E	"	10.6	6.8	12.7		1.8		—		
E	"	11.1	4.2	65.5		4.6		4.8		
E	standard error	0.75	0.61	0.65					β-Al_2O_3	Petrak et al. [6]
E		0.39	0.30	0.31					CoO	
E		0.14	0.15	0.17					CoO-MgO	
E		0.28	0.32	0.38					$CoAl_2O_3$ $MgAl_2O_3$	
E	standard error					5.18	5.16		ThO_2	Phani [7]
G	"					1.46	1.44			
E	RMS	7.0	8.5		8.5				UO_2	Boocock et al. [8]
G	RMS			3.3						
K	RMS			13					UO_2	Phani and Niyogi [9]
E	correlation coefficient	0.977	0.899			0.998				
E	χ^2	563	521	3949		515	516	516	Si_3N_4	Dutta et al. [10]
σ	rank	5	1	2	4	3			Fe	Salak et al. [11]

[a] P = value fraction porosity, b, b_1, b_2, and m = parameters

[b] E = Young's modulus, G = shear modulus, K = bulk modulus, σ = tensile strength.

[c] RMS = root mean square; rank: 1 = best, 2 = next, etc.

the starting bodies, they impact the porosity dependence over most, possibly all, of the porosity range. Further, pore character is not static and in fact commonly changes substantially with the amount of porosity, e.g. as sintering occurs, the co-ordination number of the particles increases, typically starting in the range of 6–8 at low density, but reaches 12–14 at high density [1]. Although such changes in the nature of the porosity with the level of porosity may often be greatest at low porosity levels, where their effects are more limited, this is not always so. Changes from spherical to cylindrical shaped pores can be important at high porosity [1]. Thus, models based on a single, fixed, porosity will commonly deviate from actual data, especially due to neglecting the original geometry of the models, the initial mix of porosity, or its changes with P.

Recently it has been shown that both the issue of mixes of different porosity and changing porosity can be addressed via appropriate combinations from the collection of existing minimum solid area models covering the different types of porosity commonly encountered [1]. These encompass (1) pores between particles of various stackings, and (2) pores (e.g. bubbles) contained within a matrix (e.g. as in a foam, which can be obtained by interchanging pore and solid phases) or combinations of these. Such models are based on most physical properties being determined by the minimum solid area normal to the flux or stress. For partially sintered particles this is the projection of the actual sintered area between the particles normal to the stress or flux, and for pores in a matrix, it is the projection of the minimum web area between adjacent bubbles parallel to the stress or flux [1]. Properties typically dependent on minimum solid area are those determined by local field or flux concentrations, e.g. mechanical properties and electrical and thermal conductivities. Properties not fitting such models are those mainly determined by mass (e.g. heat capacity) in which case a simple rule of mixtures of the property values for the solid and pore (e.g. air or vacuum) volume fractions should be appropriate. It was shown that in materials where actual pore structures were reasonably represented by specific pore models that the available data for mechanical properties and electrical and thermal conductivity agreed with the models [1]. It was also shown that various idealized pore structure models could be combined to account for mixes or changes of such nearly ideal porosities. Deviations of the materials from the idealized pore structures were seen as the major factor for differences between the data and models.

While the companion paper [1], dealt with idealized pore structures, this paper shows that the basic minimum solid area porosity–property trends for mechanical properties and thermal and electrical conductivity are consistent with the expected combinations of porosity types commonly encountered in bodies of more general pore structures. Since detailed porosity characterization is lacking, trends with processing–porosity character are considered and shown to be consistent with appropriate models. Support for the models is provided not only by room temperature
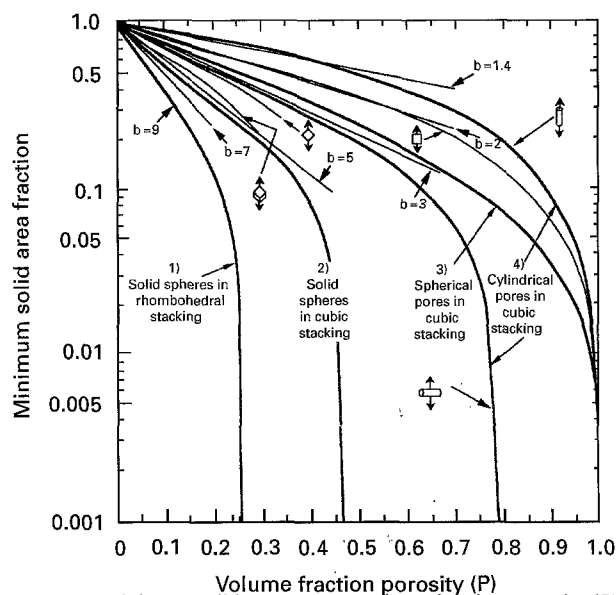

Figure 1 Minimum solid areas versus volume fraction porosity (P) calculated for various uniform stackings of perfectly uniform spherical particles or spherical, cylindrical or cubical pores. Most relative physical properties (i.e. the value at the same P divided by the $P = 0$ value) dependent on local stress or flux should be directly related to the relative minimal area, i.e. the ratio of the minimum solid area at a given P to that at $P = 0$.

dependence of the above properties of ceramics, but also for both metals and polymers. Dielectric constant is considered as a property not following minimum solid area models, instead following a rule of mixtures. Analysis and data are presented in support of this. The issue of heterogeneous porosity is addressed and illustrated.

2. Evaluation approach

The minimum solid area models that are generally most pertinent are shown in Fig. 1 (their origins and applicability to more idealized structures are reviewed elsewhere [1]). A basic characteristic of all of these models is that on a plot of the log of the property versus volume fraction porosity (P), the minimum solid area (and hence the pertinent property value of interest) decreases first, approximately, though not exactly, along straight lines on the semi-log plot. Beyond this approximately linear region on the semi-log plot of the minimum solid area and hence the property of interest starts decreasing more rapidly, then nearly precipitously, going to zero at a critical porosity (P_C). For stacked particles, P_C, the percolation limit, is where the bond area between pores goes to zero. For pores (e.g. bubbles) in a matrix it is the point at which the minimum web areas between pores goes to zero. Thus, each specific model has three characteristics: (1) the approximately linear slope of the first $\sim$40–60% of the P range to which it is applicable; (2) the $\sim P$ value at which properties start to decrease significantly more rapidly than the $\sim$ linear slope; and (3) the P_C value. While all three of these are useful in distinguishing the basic porosity character of each model, (1) is one of the more definitive and the most available [1]. The utility of each of the above three

characteristics is further enhanced by combinations of different porosity resulting in similar curves with the above three characteristic values given approximately by a weighted average of those for each type of porosity involved [1].

As previously discussed [1], various existing equations [5, 15-21] for property–porosity relations were considered to model each of the entire curves in Fig. 1 with a simple equation that contains parameters readily relatable to the pore character so that one can understand the meaning of these parameters for combinations or changes of pore structures. However, while one could obviously fit the porosity trends in one area well, this could not always reliably be done and also get a good fit to the rest of the curve. Further it is not clear that one could clearly associate the equation parameters with the porosity character in such model fitting. Thus two procedures were followed. Wherever data covered most of a model's range, comparison is made with the appropriate model curve. Otherwise (or additionally), the approximately linear character on the semi-log plot over the lower porosity region is utilized; i.e. the commonly used exponential relationship wherein the ratio of the properties at some porosity to that at zero porosity is given by

$$e^{-bP} \qquad (1)$$

where b is a parameter determined by the character of the porosity (Fig. 1). This expression has been widely used for porosity studies in the past, first on an empirical basis, then on an analytical basis by Knudsen [16] for the lower P region for different stacking of spherical particles. It was later shown to be similarly applicable to various shaped pores in a matrix [17], for which other equations had been previously derived, and has potential for being combined with the similarly derived expression pertinent only for higher porosity levels [1, 21]. Advantages of this exponential expression are: (1) it is a reasonable approximation for the actual models [1] prior to beginning the approach to P_C (lack of recognition of this deviation toward P_C and hence using this exponential model equation beyond its range of good applicability is a major source of poorer curve fitting with it); (2) there is extensive data for which the b values have already been determined; and (3) it provides a single parameter, b, which can be correlated with pore character (e.g. Fig. 1) and can be readily adapted for pore combinations via a weighted average of the b values [1]. Further, because of its mathematical simplicity, it allows ready correlation of other properties, e.g. since sound velocities are related to the square of the pertinent elastic moduli, b values for the velocities will simply be about half that of that for the corresponding modulus.

Use of the exponential relationship is consistent with studies evaluating the fit of various equations to mechanical property–porosity data showing it agrees quite well with a variety of data (e.g. being competitive with Equations 5, 6 and 7 of Table I). Further, Salak, et al.'s [11] study showed Equation 1 was, by a substantial margin, the best fit to the 834 data points for

tensile strength of sintered iron they used versus the second best fitting relationship (Equation 3 of Table I). Although not compared in detail with the other equations, they also found a good fit of Equation 1 for the 701 data points for hardness as a function of porosity of sintered iron compacts. Similarly, Enloe et al. [22] have recently considered the fit of their thermal conductivity–porosity data for AlN, as well as literature data for thermal conductivity versus porosity of Al_2O_3 and BeO. They showed that not only was the exponential relationship competitive with others considered, but it was frequently the best fitting relationship.

Use of e^{-bP} thus focuses on the slope (b) at lower P (where there is most data) as the prime discriminator of porosity type and applicable model(s). Low b values of ~ 1.4–2.7 are associated with respectively approximately cylindrical pores (aligned with the direction of measurement) and spherical pores in a matrix, both extending to very high levels of porosity (Fig. 1). Cubical pores give progressively higher b values as their orientation relative to measuring direction changes; i.e. for notation purposes, treating such pores as cubic crystals the b values for $<100>$, $<110>$ and $<111>$ directions of common pore orientation of the pores are ~ 2, 3.3 and 4.6, respectively. Such cubic pores reflect more angular characteristics of pores (e.g. from burnout of more angular fugative materials). Cylindrical pores orientated normal to the measurement direction give $b \sim 3$. The range of b values respectively for the least to most dense uniform packing of identical spherical particles is ~ 5 to 9. In general, the lower the slope (i.e. b value), the higher the transition toward P_C and the higher the P_C value. Clearly combinations must lie between the extremes of b of ~ 1.4 and 9. While characterization of porosity (beyond a density, i.e. P determination) is almost always very limited, the above P_C correlation with the pore character can imply some other aspects of porosity where investigators have covered a sufficient P range to at least begin to approach P_C.

A key problem is that even general aspects of the porosity beyond its level i.e. P, are seldom given. However, generally, variations in pore character can often be, at least approximately, related to processing. Typical die pressing of powders commonly results in lower to moderate green densities, and hence density of particle stackings, i.e. approximate random stacking of particles unless high pressures are used (in which case serious inhomogeneities such as laminations may become increasingly common. Such laminar porosity has b values similar to those for cylindrical pores of comparable orientation). Such random stacking is similar in density to simple cubic stacking of uniform spheres [1] ($b \sim 5$), e.g. it contains limited amounts of somewhat higher density stacking ($b = 6$–9), but also equal or greater amounts of voids approaching or greater than the particle size due to failure of particles to avoid bridging, i.e. voids in a matrix ($b \sim 2$–3). Considering this and pore shape (e.g. cubic pores to reflect more angular aspects of porosity), the net result would commonly be an initial b value in the range of 3 to 4. Significantly lower

b values require a much larger portion of approximately spherical or (approximately orientated) cylindrical voids. Such voids are typically obtained by introducing bubbles or fugitive, e.g. organic, particles, or due to particle bridging, and are thus often larger than the particle size of the powder particles that end up forming the body. The first of two other possibilities for low slopes (b values) is to use particles with a tendency to form chains as is commonly obtained in dealing with sols such that these leave significant interstices between the entangled chains (i.e. essentially an extreme type of particle bridging). The other possibility for low b values is use of extrusion since this can lead to some approximately aligned cylindrical porosity due to possible alignment of some particle bridges, and especially the stringing out of larger pores or organic (e.g. binder) material.

Moving further in the direction of denser packing of particles, this often results from the use of higher and more uniform pressure, via isostatic pressing. Extrusion of small bodies at higher pressure and high shear forces provides greater opportunity to reduce: (1) particle bridging (e.g. obtain better particle nesting) i.e. giving higher co-ordination number packing, hence higher density; and (2) the extent of organic (e.g. binder) stringers as sources of approximately aligned cylindrical pores. On the other hand, bodies formed by deposition of particles, e.g. by colloidal processes such as slip, tape, or pressure casting, also commonly give denser particle packing (i.e. higher green density). Hot pressing, which of course can much more readily give $P \sim 0$, frequently gives denser packings since relative particle motion commonly plays a greater role in hot pressing, especially when pressure is applied in the earlier densification stages. Similarly, Hot Isostatic Pressing of powders (as opposed to sinter-HIPing) can lead to denser packing of particles before full densification but also depends on the particles and temperature–pressure cycles.

The evaluation of data for comparison with the models presented in the next section was conducted drawing on as wide a range of data as was practical. However, some data were rejected for failing one, or (usually) more of the following three selection criteria: (1) moderate to low data scatter; (2) a reasonable extent of porosity range covered; and (3) the porosity range extending to low enough P values to give a reasonable b value. Obviously, there is an inverse dependence between the low scatter and a sufficient porosity range; i.e. more scatter can be tolerated when the porosity range is larger, and vice versa. Most data used encompassed a porosity range of 10–30% and usually in relation to other data, especially for the same investigation. Thus, data with limited porosity range and wide scatter within a given set, between sets, or both, was not used, e.g. Al_2O_3–Cr_2O_3 data [24] ($P \sim 3$ to $< 9\%$), except occasionally in conjunction with other data (i.e. in some of the figures). The location of the porosity range covered is also an issue, mainly in conjuction with the range of the porosity itself. A sufficient range of porosity over at least part of the range where the porosity dependence is transitioning from the approximately linear behaviour

on a semi-log plot to approach P_C is very valuable in defining such transitions. However, if the range of porosity is limited and does not reasonably define this transition, higher b values will be obtained which do not differentiate the models (which utilize the initial slope, i.e. extrapolated to the $P = 0$ property value). (In principle a slope other than the initial slope could be used, but such intermediate slopes are not unique to any model, and hence are not by themselves of clear use in defining the model and thus the porosity involved.) Thus, data on MgO, ZrO_2 and $CaZrO_3$ individually covering P ranges of < 2 to $\sim 6\%$, in the P range of 28–39% [25] (e.g. giving b values of 40 to > 70) were not useful for this study. As an added guide in avoiding such erroneously high b values, the $P = 0$, i.e. intercept, value of the properties are given whenever practical, since this allows comparison with other data (and is useful in and of itself).

Finally, wherever possible, b values obtained by the original investigator have been used and identified. In the many cases where b values were not available from the original study, they were calculated from the best visual fit to the data. More sophisticated data analysis was judged impractical, and not needed since, for example (a) much data is presented graphically and cannot be obtained with sufficient accuracy to justify more sophisticated analysis, (b) the above selection criteria are more important in the validity of the analysis, and (c) overall trends are being sought, so moderate deviation for individual sets of data are not particularly significant where several sets of data are involved. No significant deviations between trends for b values calculated by the original investigator(s) or this author were found, and calculations by this author agreed with values of the original investigators on their data.

3. Comparison of property porosity data with the models

3.1. Ceramics

Table II presents the results of an extensive survey of the porosity dependence of tensile strength and especially elastic properties of various ceramics at room temperature. Table III summarizes the much more limited data for hardness and compressive strength of ceramic materials versus porosity at room temperature, and Table IV summarizes data for thermal and electrical conductivities of various ceramics versus porosity at or near room temperature. This data is further summarized (Table V) for various methods of powder consolidation where these were identified. The first of two key results of this extensive survey is that the overall average b value for a wide variety of materials and processing is ~ 4. This is as expected from Fig. 1, since this is the approximate average over all models. The second key result of this survey is that there is some differentiation of b values with different consolidation methods and this is consistent with the expected trend in porosity character with these different methods. Thus, hot pressing consistently gives higher b values than does cold pressing with iso-pressing and colloidal processing also tending to give higher

TABLE II Summary of ceramic elastic and tensile strength property–porosity data

No.	Material	Investigator	Proc.[a]	P(%/μm)[b]	GS(μm)[c]	No. Meas.[d]	b[e] slope values for: E — b(E_0 in GPa)	G — b(G_0 in GPa)	Other — b(M_0)[f]
	(A) Single Oxides								
1	Al_2O_3	Coble and Kingery [26]	SC (FG)	15–55	23	5–50	2.8 (390)	2.8 (1.64)	4 ($\sigma_0 = 250$) 0 ($\nu_0 = 0.27$)
2	Al_2O_3	De Portu and Vincezini [4]	TC	8–31		~30	4.1[f] (420)		
3	Al_2O_3	Wang [27]	CP	5–43		40 D&S	4 (400)		
4	Al_2O_3	Sztankovics [28]	Iso ex.	0.1–14.4	0.7–12	9	3.2 (340)		7.2[f] ($\sigma_0 = 540$)
5	Al_2O_3	Neuber and Wimmer [29]	S	3–18		16	2.9 (280)		
6	Al_2O_3	Binns and Popper [30]	CP	1–10	15–50	10			
7	Al_2O_3	Green et al. [31]	CP	20–50		13	4.5–5.5		
8	Al_2O_3	Wu and Rice [32]	HP	2–40	≤1	4–10	2.6 (400)		2.2 ($K_{ICO} = 4$)
9	B_6O	Petrak et al. [33]	HP	0–8			4.0 (475)	4.0 (206)	5 ($\sigma_0 = 360$) 0 ($\nu_0 = 0.155$)
10	BeO	Chandler et al [34, 35]	EX	2–17			2.3 (410)	2.2 (145)	3· ($\sigma_0 = 500$)
11	BeO	O'Neill and Livey [36]	CP	0–7			3.7 (400)		4 ($\sigma_0 = 350$)
12	BeO + 8% SiC	O'Neill [23]	CP	0.5–4	50–100	8	2.8 (400)		
				3–7	2–18	11	3.4 (400)		
				0.5–3	7–20	24	3.4 (400)		
13	CeO_2	Argoitia et al [37]	CP	3–9	~20	14	2.8 (205)		
14	CoO	Petrak et al. [6]	CP	9–20	35	8	4.5[a] (230)		
				6–16	40	8	4.4[b] (260)		
15	CaO-MgO / HfO_2 (+20m/o Er_2O_3, Gd_2O_3)	Hunter et al. [38]	HP	4–24		8	4.5 (245)	3.9 (96)	
16	HfO_2 (+33m/o Er_2O_3)	Dole and Hunter [39]	CP	0–18	20–40	8	2.3 (240)	2.1 (94)	
17	Pr_6O_{11}, Tb_4O_7 / HfO_2 (+1m/o Er_2O_3)	Hunter et al. [40]	HP	2–18			4 (270)	3.7 (105)	
18	HfO_2 (U)	Dole et al [41]	HP	4–24		13	4.3 (285)	4.1 (110)	6 ($B_0 = 235$)
19	MgO	Spriggs et al [42]	HP	0–24		≥20	4.7[e] (320)	4.9[e] (140)	
20	MgO	Janowski and Rossi [43]	HP	0.2–11.5		14	4.1 (305)		
21	MgO	Biddulph [44]	CP	~5–30		~100	3.7 (270)		4.6 ($\sigma_0 = 130$)
22	Nb_2O_5	Manning [45]	HP	~0–18		24	5.1 (150)		
23	Dy_2O_3	Manning et al. [3]	CP, IP	3–19		22	2.8[e]–(170)	2.6[e]–(64)	
24	Er_2O_3	Manning et al [3]	CP, IP	5–21		27	2.9[e]–(180)	2.9[e]–(70)	
25	Gd_2O_3	Haglund and Hunter [46]	CP	2.5–36.7			4.1 (310)		0 ($\nu_0 = 0.28$)

TABLE II (Continued)

No.	Material	Investigator	Proc.[a]	P(%/μm)[b]	GS(μm)[c]	No. Meas.[d]	b^e slope values for:		
							$b(E_0$ in GPa) E	$b(G_0$ in GPa) G	Other $b(M_0)^f$
	(A) Single Oxides (contd)								
26	Ho₂O₃	Manning et al [3]	CP, IP	1–18		21	2.6[b]–(170)	2.6[e] (67)	
27	Lu₂O₃	Hunter and Graddy [47]	CP	3–33			4.2 (193)	4.1 (75)	
28	Sm₂O₃	Hunter et al. [48]	CP	2–37		15	3.5 (145)	2.7 (55)	0.4 ($v_0 = 0.32$)
29	Sm₂O₃	Dole et al. [49]	CP, IP	2–24			5.6 (145)	4.9 (55)	
30	Tm₂O₃	Dole et al. [49]	CP, IP	2–24			3.3 (180)	4.2 (69)	
31	SiO₂	Harris and Welch [50]	CP	1–18			3.2 (70)		
32	SiO₂	Tomilov [51]	SC	1–19		16	5.4 (70)		2.0 ($\sigma_0 = 110$)
33	SiO₂	Park and Hench [52]	gel	0–55					
34	ThO₂	Spinner et al. [12]	IP	7–40 / 4–33			4 (260) / 6 (260)	6 (100) / 6 (100)	2.7 ($\sigma_0 = 180$)
35	ThO₂	Curtis and Johnson [53]	CP	5–41	~ 60	8	3.4 (280)	3.5 (85)	
36	UO₂	Boocock et al. [8]	CP	0.7–28		43	3.3 (225)		
37	UO₂	Panckkal and Ghosh [54]	CP	5–10		17	4.1 (270)		
38	Y₂O₃	Marlowe and Wilder [55]	IP	5–37	0.3–220	12	4.4 (180)		
39	Y₂O₃	Manning et al [3]	CP, IP	4–22		17	2.8[e] (180)	2.7[e] (69)	
40	ZrO₂	Smith and Crandall [56]	HP	5–18		7	4.2 (250)	4.7 (97)	
41	ZrO₂ + 33m/o P₆O₁₁	Dole and Hunter [39]	CP	0–12		5	2.6 (225)	2.3 (89)	
42	ZrO₂ + 33m/o Tb₄O₇	Dole and Hunter [39]	CP	5–12		6	2.6 (225)	2.3 (89)	
	(B) Mixed oxides								
1	β-Al₂O₃	Evans et al. [57]	IP	1–38		10	5.0 [14] (215)		7 ($\sigma_0 = 275$)
2	CoAl₂O₃	Petrak et al. [6]	CP	3–14 / 1–16	5–100	16	5.4[e] (225) / 3.1[e] (280)		
3	Li₄SiO₄	Chu et al. [58]	CP	7–32	4–400	3	3.9[e] (140)	3.8[e] (55)	
4	MgAl₂O₄	several [59]		0–32		> 30	5.4[e] (285) / 3.1 [15] (280)		
5	MgAl₂O₄	Porter et al. [60]	HP	1–32		12	4.1[e] (300)	4.0[e] (120)	4.7[e] ($B_0 = 215$)
6	MgAl₁.₆Cr₀.₄O₄	"	HP	3–20			4.1[e] (270)	4 (110)	4.2 ($B_0 = 176$)
7	MgAl₁O₈CrO₀.₆O₄	"	HP	3–20			5.1[e] (310)		5.5 ($B_0 = 215$)

TABLE II (Continued)

No.	Material	Investigator	Proc.[a]	P(%/μm)[b]	GS(μm)[c]	No. Meas.[d]	b[e] slope values for: E — b(E_0 in GPa)	G — b(G_0 in GPa)	Other — b(M_0)[f]
(B) Mixed Oxides (contd)									
8	$MgAl_{1.0}O_8$		HP	3–20			3.8[e] (257)	3.7[e] (101)	4.5 (B_0 = 183)
9	$Cr_{1.2}O_4$ $MgAl_0O_4$	„	HP	3–20				3.7[e] (92)	4.2 (B_0 = 158)
10	$Cr_{1.6}O_4$ $MgAl_{0.5}Fe_{0.5}O_4$	„	HP	3–20		7	4.4[e] (230)	4.2[e] (90)	5.8[a](B_0 = 179)
11	$MgCr_2O_4$	„	HP	5–25		35	4.7[e] (225)	4.5[e] (90)	5.8[a] (B_0 = 170)
12	Mullite	Penty et al. [61]	HP, S	~1–13		10	3–3.5 (230)		4.7 (σ_0 = 150)
13	Mullite	Metcalfe and Sant [62]	CP	~1–20.5					
14	SrO-FeO	Wills and Masulancia [63]	CP	6–17		6			3.4[g]
15	$YBa_2Cu_3O_7$	McAlford et al. [64]	EX	1–24		27	3.7 (180)		
16	$YBa_2Cu_3O_7$	Bridge and Round [65]	CP	3–42		8	4.2 (9)	4.6 (40)	4.0 (B_0 = 52)
(C) Non-oxides									
1	B	Petrak et al. [33]	HP	0–30	~2	9			3.2[e] (350)
2	TaB_2	Claussen [66]	HP	1–25			5.0[e] (445)		3.2[e] (σ_0 = 440)
3	TiB_2	King and Wheldon [67]	HP	3–20					
4	TiB_2	Mandorf and Hartwig [68]	HP	3–20			3.7[e] (546)		3.2[e] (σ_0 = 284)
5	POCO Graphite	Cost et al. [68]		13–32		24	3.5[e] (255)	3.3[e] (97)	1 (ν_0 = 0.31)
6	B_4C	Liebling [70]	HP	0–9			5.7[e] (480)		
7	B_4C	Champange and Anger [71]	HP	8–30	18		5.5[e] (280)	5.7 (204)	
8	B_4C	Beauvy [72]	HP	0–30			5.0[e] (445)		
9	B_4C	Wu & Rice [32]	HP	0–15		6–17	4[e] (500)		3.9 (σ_0 = 500)
10	B_4C + O-3%C	Schwetz et al. [73]	S, HIP	0.4–3.2 0.4–24.6	5–10	5	3.4 (435)	3.8 (190)	2.6 (σ_0 = 440)
11	B_4C	King and Wheildon [67]	HP	1–25					3.4 (σ_0 = 510)
12	B_4C	Hollenberg and Walther [74]	HP	0–15		> 10	4.2		
13	B_4C	Osipov et al. [75]	HP	~0–45	5	7			2.9 (σ_0 = 750)
14	Cr_3C_7	Knudesn [76]	HP	0.3–20	6–10 8–12 9–15 9–15				6.6[e] (σ_0 = 1580) 5.8[e] (σ_0 = 1580) 4.6[e] (σ_0 = 1580) 4.4[e] (σ_0 = 1580)

TABLE II (Continued)

No.	Material	Investigator	Proc.[a]	P(%/µm)[b]	GS(µm)[c]	No. Meas.[d]	b[e] slope values for: E, b(E0 in GPa)	G, b(G0 in GPa)	Other, b(M0)[f]
	(C) Non-oxides (contd)								
15	SiC	Gulden [77]	CVD	0.1–8		43			7 ($\sigma_0 = 800$)
16	SiC	Coblenz [78]	S, HP	<1–15		3.2e (470)			
17	SiCβ	Broussaud et al. [79]		0–49	≤5	15			4.5 ($\sigma_0 = 600$)
	SiCα			0–10	5 > 20	14			3.0 ($\sigma_0 = 360$)
18	SiC	Carnahan [80]	HP	~0–15	≥7	6	4.2 (448)		
19	SiC	Procharzak et al. [81]	S	3–28		14		4.3 (192)	3.0 ($\sigma_0 = 652$)
20	SiC	Seshardi et al. [82]	S	1–7		25–50	2.2e (420)		1.8 ($K_{\text{ico}} = 4.4$)
21	SiC	Croixet et al. [84]	HP	2–27		6	4.9 (440)		
22	ZrC	Bulychev et al. [85]	EX	1–32	10–25	40			~5 ($\sigma_0 = 520$)
23	AlN	Boch et al. [85]	HP	0–20		18	5.5 (310)	5.7 (130)	0.9 ($\nu_0 = 0.24$)
24	Si3N4	Datta et al. [10]	RS,S,HP	0–38		> 450	3.3e (300)		
25	Si3N4	Bubnov et al. [86]	HP	0–40			4 (300)		
26	Si3N4	Fate [87]	HP,S	0–27		8		3.2 (125)	
27	Si3N4	Yeheskel and Gefen [88]	HIP,S	0–36			5 (310)		
28	Si3N4	DePorto and Vincenzini [89]	HP	0–35		13	5.7 (290)		
29	Si3N4	Larson et al. [90]	S, RS	1–27		~25	3.1 (315)		3.9 ($\sigma_0 = 400$)
30	Si3N4	Rice [91]	RS; S [91, 92]	0–45		>100 (survey)			
31	HfN	Desmaism-Brut et al. [92]	IP	5–15	–	3	5.2 (550)	4.6 (220)	0.6 ($\nu_0 = 0.26$)
32	TaN	"	IP	1–15	–	4	4.6 (515)	3.5 (205)	0.6 ($\nu_0 = 0.25$)
33	TiN	"	IP	1–22	–	4	3.0 (475)	2.8 (195)	0.2 ($\nu_0 = 0.22$)
34	ZrN	"	IP	2–8	–	4	3.3 (390)	3.7 (155)	0.8 ($\nu_0 = 0.26$)
35	Si2N2O	Boch and Gandus [93]	HP	0–27		16	3.7 (220)	3.5 (90)	

[a] Proc. = Processing, SC = slip cast, (FG = fused grain used), TC = tape cast, CP = cold-pressed, iso. ex = isostatic extrusion, ex = extruded, IP = iso-pressed, gel = made via sol-gel processing, s = sintered (shown only where no other data available; i.e., implied for other forming processes, such as SC, TC, CP, etc.); HP = hot-pressed, HIP = hot isostatically pressed, RS = reaction sintered.

[b] P = porosity (given in %), also typical size (in µm) shown where available.

[c] GS = grain size.

[d] No. meas. = number of measurements.

[e] b values determined by the original investigator.

[f] σ_0 = tensile (or flexure) strength at $P = 0$ (in MPa); B_0 = bulk modulus at $P = 0$ (in MPa), K_{ICO} = fracture toughness at $P = 0$ (in MPa m$^{\frac{1}{2}}$) and ν_0 = Poisson's ratio at $P = 0$.

[g] Relative strengths, absolute values not given.

TABLE III Hardness, compressive strength–porosity data

No.	Material	Investigator	Proc.[a]	P(%/μm)[b]	GS(μm)[c]	No. Meas.[d]	b (slope values for:) H_v[e] $b(H_0$ in GPa)/load (kg)	Other Hardness[f]	Compressive Strength (C) $b(C_0,$ GPa)[g]
1	Al_2O_3	Neuber and Winimer [25]	S	3–18	~6	16	5.5 (29)		
2	Al_2O_3	Wu and Rice [32]	HP	0–40	≤1	3–9	6.3 (22)/?	S:6 (27)	5.4 (1.8)
3	B_6O	Petrak et al. [33]	HP	1–22		≥13			7.3 (1.4)
4	BeO	Udy and Bougler [94]	?	2–31		>7			
5	BeO	Elston and Labbe [95]	HP	1–6		6			7.4 (2.3)
6	SiO_2	Park and Hench [52]	gel	0–55	–	4	3.2 (65)/?		1.8 (0.48)
7	Y_2O_3	Helferich and Zanick [96]		3–30	38		3(23)/0.3		
8	Al_2O_3–Cr_2O_3	Cho et al. [97]	CP	3–48	1–30	38	3(23)/0.3		
9	$MgAl_2O_4$	Budnikov et al. [98]	HP	0–22	2–10	11	2.7 (11.6)/0.1		
10	PZT	Okazaki and Nagota [99]	HP	2–13	3–4	4	5.8 (4.5)/?		
11	TiB_2	Gropyanov et al. [100]		0–30	1–5	30		RA: 1.5 (95)	
12	TiB_2	Mandorf and Hartwig [68]	HP, CP	6–15		3			4.5 (2.2)
13	Glassy C	Hucke [101]		45–70	–		3.2(4.3)/1		
14	Glassy C	Hucke [101] and others [14]	–	31–70	–	>50			3.3 (1.4)
15	B_4C	Wu and Rice [32]	HP	0–14		6	5.3 (40)/1	S:6.6(140)/1	3.7 (910)
16	B_4C	Osipov et al. [75]	HP	0–45	5	7			
17	SiC	Croix et al. [83]	HP	2–40		10	6.4 (40)		
18	TiC	Yamada et al. [102]	HP	4–11	~20	11	5.8 (35)/?		
19	AlN	Boch et al. [85]	HP	1–20	20	10, 5	7.7[a] (15.6)/1, 6.3[a] (11.5)/1		
20	Si_3N_4	Mukhopadhyay et al. [103]	S	0–1	50	18	4.2[a] (16.4)/?		

a Proc. = Processing, SC = slip cast, TC = tape cast, CP = cold-pressed, iso. ex = isostatic extrusion, ex = extruded, IP = iso-pressed, gel = made via sol-gel processing, s = sintered (shown only where no other data available; i.e., implied for other forming processes, such as SC, TC, CP, etc.); HP = hot-pressed, HIP = hot isostatically pressed, RS = reaction sintered.

b P = porosity (given in %), also typical size (in μm) shown where available.

c GS = grain size.

d No. meas. = number of measurements.

e Vickers hardness, H_0 = hardness at $P = 0$, loads used shown in kg (? means no load given); superscript a designates b values determined by the original investigator.

f S = scratch, RA = Rockwell A, values in parentheses are at $P = 0$.

g C_0 = compressive strength at $P = 0$.

TABLE IV Summary of ceramic thermal and electrical conductivity–porosity data

No.	Material	Investigator	Proc.[a]	P^b(%)	No. Meas.	b^c (slope values) for conductivity
	(A) Thermal conductivity					
1	Al_2O_3	Gardner et al. [104, 105]	HP	0–50	20	4.62
2	BeO	Murray [106]	S?	3–50	5	2.5
3	BeO	Nat. BeO [107, 108]	S	4–45		4
4	BeO	Powell [109]	HP, S	0–30	6	3.2
5	BeO	Elston and Labbe [94]	HP	5–43		4.5
6	UO_2	Hobson et al. [110]	S	1–9	4	2.5
7	UO_2	Van Craeynest and Stora [111]	S	1–9	6	3.1
8	UO_2	Moore and McElroy [112]	S?	0–7	3	1.3
9	UO_2	Ross [113]	S	1–23	6	1.6
10	Silicon Marl	Saegusa et al. [114]	–		4	1.8
11	Sandstone	Sugawara and Yoshizawa [115]	–	10–40	16	2
12	Graphite	Wagner et al. [116] Rhee [117, 118]	–	15–40	6	2
13	AIN	Enloe et al. [22]	HP, S	0–40	> 30	4[a]
	(B) Electrical conductivity					
1	ZrO_2	Rutman et al. [119]	CP	6–50	5	2.9
2	TiC (Fibres)	Samsonov and Matsera [120]	Ex	5–30		1.7 (360 μm dia)[d] 1.8 (490 μm dia)[d]
3	ZrC	Bulychev et al. [121]	Ex	1–30	> 65	2.1
4	C	Belskaya and Tarabanov [122]	Ex	0–70	6	1.8

[a] Processing: HP = hot pressing, S = sintering, (? means this is assumed from description in paper rather than explicitly stated), – means there are no indications of processing in the referenced work, CP = cold-pressed (then sintered), Ex = extruded.
[b] P = porosity.
[c] Superscript a designates b values determined by original investigator.
[d] Fibre diameters in parentheses.

TABLE V Summary of ceramic property–porosity dependence for different processing[a]

| Property | b Values | | | | |
	Extruded	Cold-pressed	Iso-pressed	Colloidal	Hot-pressed
Young modulus (E)	1.7 ± 0.4 (2)[b]	3.6 ± 0.8 (25)	4 ± 0 ± 1.2 (14)	3.9 ± 1.2 (4)	4.5 ± 0.7 (31)
Shear modulus (G)	2.2 (1)	3.2 ± 0.9 (8)	3.9 ± 1.3 (12)		4.3 ± 0.6 (17)
Bulk modulus		4.0 (1)			5.1 ± 0.8 (8)
Tensile strength (σ)	5.1 ± 2.1 (3)	4.0 ± 1.1 (3)	7(1)	4(1)	4.5 ± 1.3 (12)
Hardness (H)		4.1 ± 1.1 (5)			5.8 ± 1.4 (8)
Compressive strength	–				5.8 ± 1.5 (3)
Thermal conductivity (K)	2.5 ± 1 (6)				4.4 ± 0.3 (3)
Electrical conductivity	1.9 ± 1 (4)	2.9 (1)			

[a] Values shown are averages and ± 1 standard deviation where more than value was available.
[b] Values in parentheses = number of studies average.

b values than cold pressing, as expected. This trend for higher b values for iso-pressed versus cold-pressed bodies is reinforced by the fact that the b values for Young's modulus for samples that were only iso-pressed and not previously die-pressed is higher than bodies that were first cold-pressed then subsequently iso-pressed (i.e. some of the lower density structure from die pressing, e.g. laminations, is often difficult to remove by iso-pressing). Also note similar b values for both thermal conductivity and Young's and shear moduli of the various ceramics with a possible tendency for somewhat higher values for tensile strength and especially hardness (consistent with earlier studies [1,14]).

The above survey trends are reinforced, and additional trends are shown by reference to individual studies, singly or in groups. Thus, combining different investigators' data for the same materials, typically gives average b values of ~4 (e.g. Figs 2 and 3). More extensive surveys, e.g. that of Al_2O_3 [123] (encompassing 50–100 data points) give similar values. However, uncertainties can still remain in intercepts at $P = 0$ as well as in where significant deviation from the linear semi-log trend toward P_C occur. For properties not significantly dependent on grain size or other microstructural factors, e.g. elastic moduli, polycrystalline values obtained from single crystals [123] or
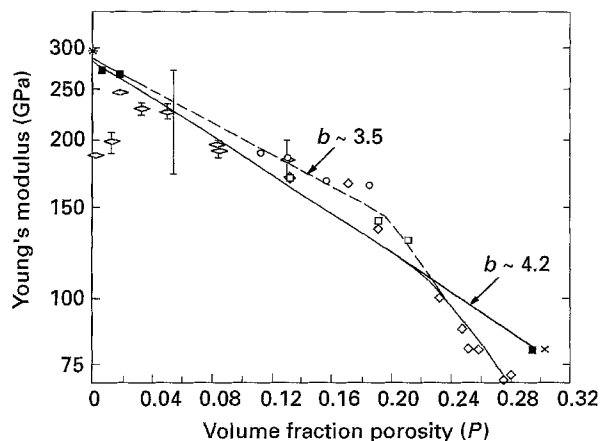
Figure 2 Young's modulus versus volume porosity (P) for various $MgAl_2O_4$ bodies at $22\,°C$. Most bodies were made by sintering, usually via cold pressing (CP). However, those of Chay et al. [130] and Petrak et al. [6] were made by hot-pressing (HP). Vertical bars represent the range of data (for Bailey and Russell [129]) or the standard deviations (Chay et al). Note: (1) the reasonable agreement between the polycrystalline value computed from single crystal measurements with the extrapolation of the $E - P$ data to $P = 0$, and (2) different (higher) b value (heavier solid line) and resultant greater scatter if all data is averaged versus focusing on one set of data, e.g. Chung et al.'s [127] (dashed and lighter solid line) are considered. × Wachtman and Lam [126] (S); □ Terwilliger [128] (S); ○ Schreiber [59] (S); ◇ Chung et al. (S); ■ Lang [125] (CP, HP); I Bailey and Russell [129] (S); ◇ Chay et al. [130] (HP); * Chung and Buessem [124].

Figure 3 Young's and shear modulus versus volume fraction porosity (P) for various MgO bodies at $22\,°C$. Data of Janowski and Rossi [43] for hot-pressed (HP) specimens tested as fabricated as well as after one year exposure to the atmosphere are shown along with data from a variety of other investigators utilizing hot pressing or sintering with consolidation via either cold pressing (CP) or slip-casting (SC). Again note the differing trends, e.g. b values, if all data is averaged versus individual sets of data for a given investigator and processing. Janowski and Rossi [43] : □ as hot-pressed; ■ exposed to atmosphere for 1 year. ● Spriggs (HP); + Lang [125] (CP); ⊙ Schwartz (SC); △ Wachtman (CP); ○ Tinklepaugh (HP); ⊕ Wyant (SC); × Chung and Buessem [124] (xl).

dense glasses of the same composition as the porous bodies can be of great value in establishing $P = 0$ intercepts and in better defining the deviation from semi-log linearity toward P_C (e.g. Figs 2–5). Unfortunately, these are not used near enough. Fig. 4 shows the b value shift with and without use of such $P = 0$ values (see also Figs 2 and 8).

Another overall trend corroborated by this survey is for higher b values (initial slopes) to be generally associated with lower P_C values, as expected, and their association with cited processing trends (e.g. Figs 2–8), Thus, slip casting of fused SiO_2 by Harris and Welsh [50] and Tomilov [51] (Fig. 5) leads to low P_C values, e.g. < 0.14 and ~ 0.2, with higher b values of ~ 5.4 while Harris and Welsh's data for slip cast foamed SiO_2 has a substantially lower b value and a higher P_C value consistent with the presence of considerable approximate spherical porosity. Sintered MgO data of Lang [59,124–128,133] also shows moderate b values for shear (G) and Young's (E) modulus of MgO with $P_C > 0.24$ and probably > 0.3, whereas hot-pressed data of Spriggs et al. [42] and Janowski and Rossi [43] clearly show a higher b value (Fig. 3). Similarly, the data for sintered $MgAl_2O_4$ [125–129] indicates the decrease towards the P_C value beginning at $P < 0.3$, consistent with an average b value when the significant deviations of the data of Chay et al. [130] are recognized by comparison with other, e.g. single crystal [124], data. More definitive is the work of Green et al. [31] showing increasing b values and decreasing P_C values for bulk (B), shear, and Young's modulus of cold-pressed Al_2O_3 (Fig. 6). This is further reinforced when their data is combined with much earlier similar data of Wilcox and Cutler, i.e. showing increasing b and decreasing P_C values with increasing
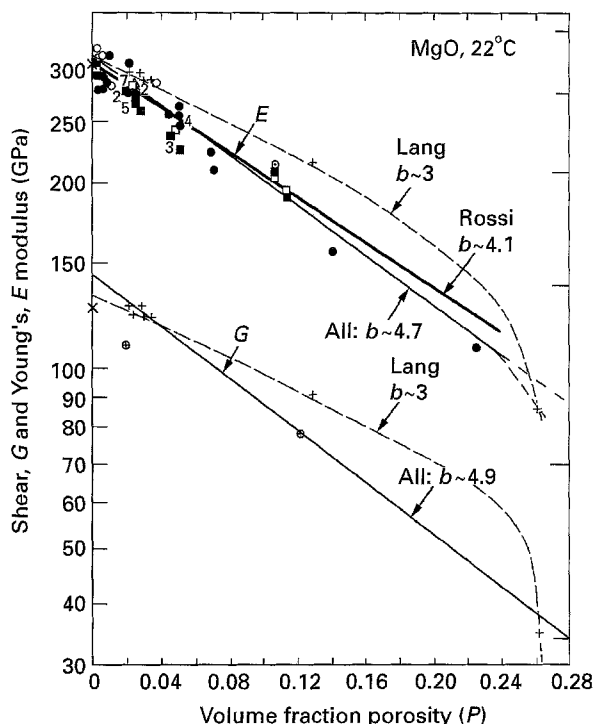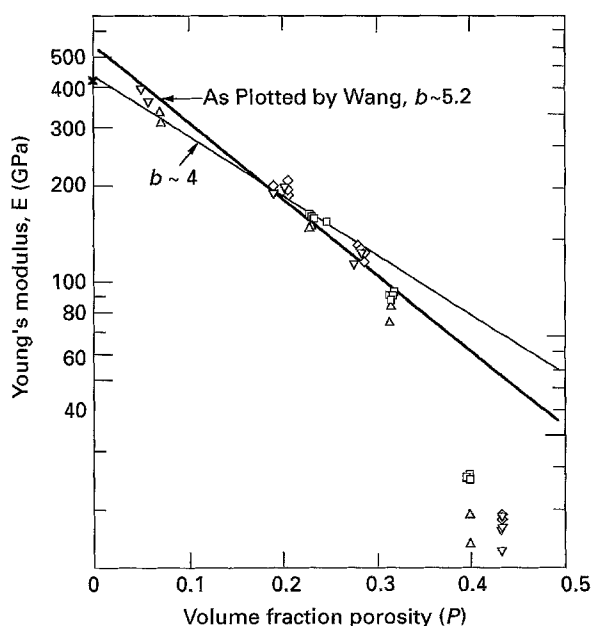

Figure 4 Comparison of Wang's [27] Al_2O_3-P Young's modulus data with single crystal (sapphire) [12] data. Note that the latter shows Wang clearly overestimated the slope (b value) of his data; which, in turn, even more clearly shows the property deviation below the linear trend at lower P. × Chung and Buessem [124] (xl); Wang [27] : □ 100 series (sonic); ◇ 300 series (sonic); △ 100 series (bending); ▽ 300 series (bending).
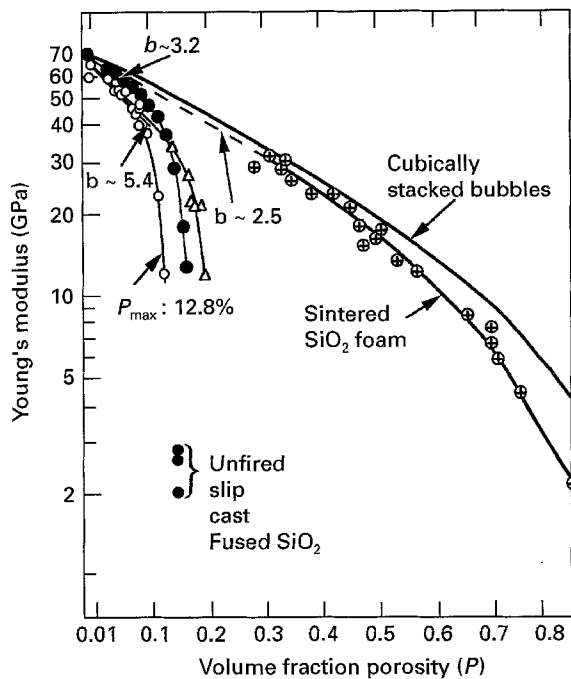
Figure 5 Young's modulus versus volume fraction porosity (P) for sintered fused quartz at 22 °C. Data of Harris and Welsh [50] and Tomilov [51] (for two different methods of preparation) for slip-casting of bodies. Note the expected inverse trends for b and P_C. △, ○ Tomilov [51] ; ●, ⊕ Harris and Welsh [50] ; ● unfired slip cast fused SiO₂.
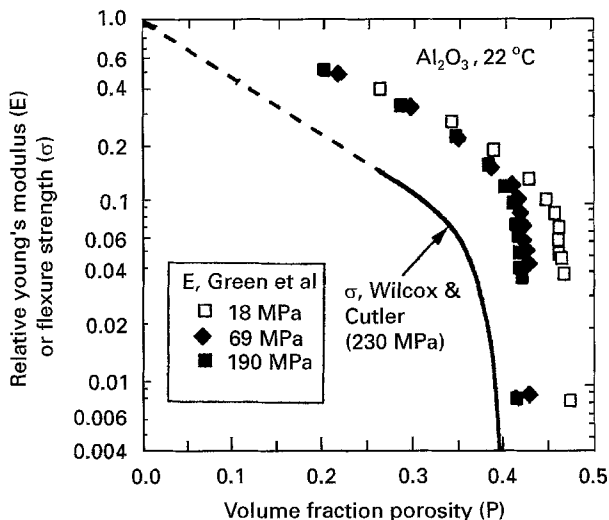

Figure 6 Relative Young's modulus and flexure strength versus porosity data for respectively die-pressed Al₂O₃, 22 °C. Data of Green *et al.* [31] and σ, Wilcox and Cutler [131] for differing (listed) compaction pressure. Note the expected decrease in P_C values with increasing pressure. Green *et al.* [31] ; □ 18 MPa; ◆ 69 MPa; ■ 190 MPa.

Figure 7 Relative Young's, shear, and bulk moduli along with relative electrical and thermal conductivities of various graphite and carbon bodies at 22 °C. Note the lower slope (b value ~ 1.8) and greater P_C value (> 0.7) for the extruded material of Belskaga and Tarabanov [122] versus a higher slope and lower indicated P value for typical pressed bodies [116–118]. Note also the excellent overall agreement of the various properties for the latter, and that the scatter probably reflects porosity variations (inhomogeneity). ● Belskaya and Tarabanov [122]; Wagner and Rhee *et al.*: □ E/E_0, G/G_0, B/B_0; + C/C_1; × K/K_0.
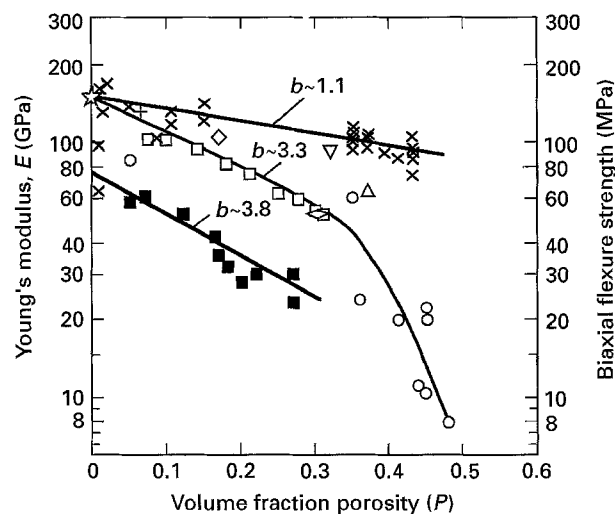

Figure 8 Young's modulus and biaxial flexure strength versus P for YBa₂Cu₃O₇₋ₓ, 22 °C from various investigators [64,65,138–142] (see Lewis' [137] compilation). Ex = extruded, CP = cold-pressed, TC = tape case, and ? = uncertainty in processing. Note a distinctly lower slope (b value) for extruded versus cold-pressed bodies and the corresponding lower P_C value for the latter. Note also the P = 0 E value from averaged single crystal values [139–141]. Eσ E×: Alford *et al.* (Ex); ○ Bridge and Round [65] (CP); ☆, ▽ Ledbetter *et al.* [139] ; □ Singh *et al.* (CP); △ Round and Bridge [142] (CP?); + Almond *et al.*; ◇ Tallon *et al.*; <> Kusz and Murawski, ■ Singh *et al.* (TC).

pressing pressure as expected from resultant denser particle packing [131]. Such b versus P_C and processing trends are also shown by the relatively low slope (~1.8) for relative electrical conductivity of extruded carbon of Belskaya and Tarabanov [122] and the high P_C value (> 0.7) versus the higher slope (~2.3) and lower P_C (~0.4) for carbon and graphite bodies typically made by cold pressing (Fig. 7). Lower b values with extrusion versus cold pressing, the similarity of σ − P and E-P behaviour (especially in view of the

somewhat higher σ b value being consistent with those specimens being tape cast), and the use of single crystal derived P = 0 polycrystalline E values are all shown by a compilation of YBa₂Cu₃O₇ − x data [64, 65, 137–142]. While extrusion might effect properties by producing preferred orientations, this is not the major cause of the difference between the porosity dependence of extruded versus other materials. First other forming processes can produce preferred orientation, though often less than extrusion. Second, significant preferred orientation would shift the whole

property–porosity curve; i.e. including its $P = 0$ intercept (which is not observed). Finally, as noted earlier, b values for sound velocities should be about half the values for the corresponding elastic property. Thus, for example, sound velocities of cold-pressed and sintered UO_2 having a b value of 2.1 [132] are consistent with elastic property dependence of such processing.

3.2. Other materials and overall trends

Relative room-temperature thermal conductivity for some fire bricks and mainly sedimentary rock specimens predominantly show b values of ~ 2 and correspondingly high P_C values of the order of 0.6 to > 0.8, consistent with an expected significant fraction of approximately spherical, tubular (or laminar porosity) [1, 113, 114]. Substantial relative Young's modulus and tensile strength data of various pressed and sintered metals, mainly by Jernot et al. [133], along with some Fe data by McAdam [134], are generally consistent with the trend for cubic (hence random) stacking of uniform spherical particles expected for typical die pressing (Fig. 9). The deviation toward lower b values than for cubic or random stacking of uniform spherical particles is consistent with the expected presence of approximately-spherical pores resulting from bridging due to varying particle size. Pohl's [135] compilation of E–P data for iron made by various routes confirms different porosity dependencies for different processing and resultant different pore structures. This agreement of metal data with the minimum solid area models is strongly reinforced by Salak et al.'s [11] showing that the exponential relationship was by a substantial margin the best fit to the 834 tensile strength data points for sintered iron they used with a resultant b value of ~ 4.3, as well as showing a good fit to this relation for the 701 data points or hardness of sintered iron, giving a b value of ~ 4.9. Similar results are seen for relative electrical conductivity for the same and similar metals in data of Jernot et al. [133] (Fig. 10), again corroborating similar porosity dependencies for mechanical properties and electrical conductivity. While no data for properties of polymers with general pore structures is known, data of Phani and Murkerjee [136] for approximately spherical pores in cast polymers has previously been shown [1] to be in good agreement with the minimum solid area for spherical pores (i.e. b values of ~ 3).

The above results for other materials (i.e. rocks, metals and polymers) corroborate all of the trends for ceramics (previous section). The common trends for mechanical properties and thermal and electrical conductivities with pore character across a range of materials corroborate the common porosity dependencies for such stress and flux dependent properties. This was also found for bodies with porosities of approximately ideal pore structure [1]. This commonality for different materials, e.g. metals and ceramics, is important in considering possible variations of different mechanical properties (discussed later). Finally, it is important to note that there are clearly processing–porosity character dependences of properties, e.g. Figs 2, 3, 5–10. Other data also show this, e.g.
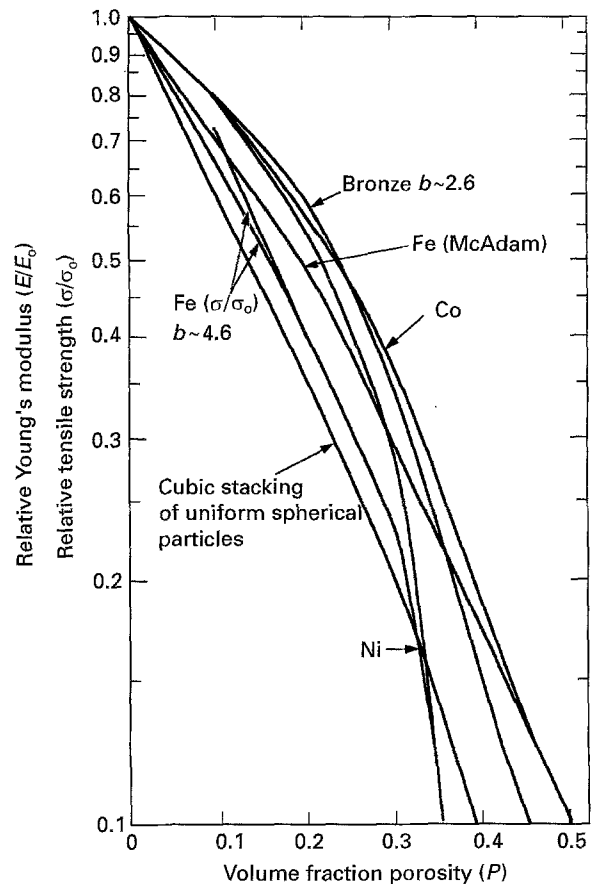

Figure 9 Relative Young's modulus or tensile strength versus P (at 22 °C) for various metals. Note reasonable agreement with the trends for cubic (hence also an approximately random) packing of spherical particles. Most data from Jernot et al. [133], but Fe data from McAdam [134].

in Larson et al.'s [90], compilation of SiC–P data gave an overall $b \sim 2.8$, but separation of reaction processed versus normally sintered SiC gave respectively b values of ~ 1.7 and ~ 3.2 (a typical value for die pressed and sintered material), i.e. a distinctly lower value for reaction processing. This is consistent with previous observations of properties from other processing methods also following very similar trends for existing models, but showing the need for refinement of the changes of minimum solid area with P for different processing methods [1].

Detailed evaluation of other models is not practical here, but key issues regarding the composite sphere models [143,144], which have received substantial attention, should be noted. First, earlier derivatives of this approach by Rossi and Hasselman have been shown to be less accurate than the minimum solid area approach (see, respectively, [145] and Table I, column 3). Second, assumptions of these models, namely, that (a) the application of a hydrostatic pressure to the composite sphere assemblage can adequately represent the stress and strain response to other stresses and that the pressure is uniformly experienced by all of the various hollow spheres comprising the model body, and (b) Poisson's ratio (v) can either increase and decrease with increasing P, with it converging to a fixed value at $P = 0.5$ or 1, are open to question. The level and distribution of stresses and
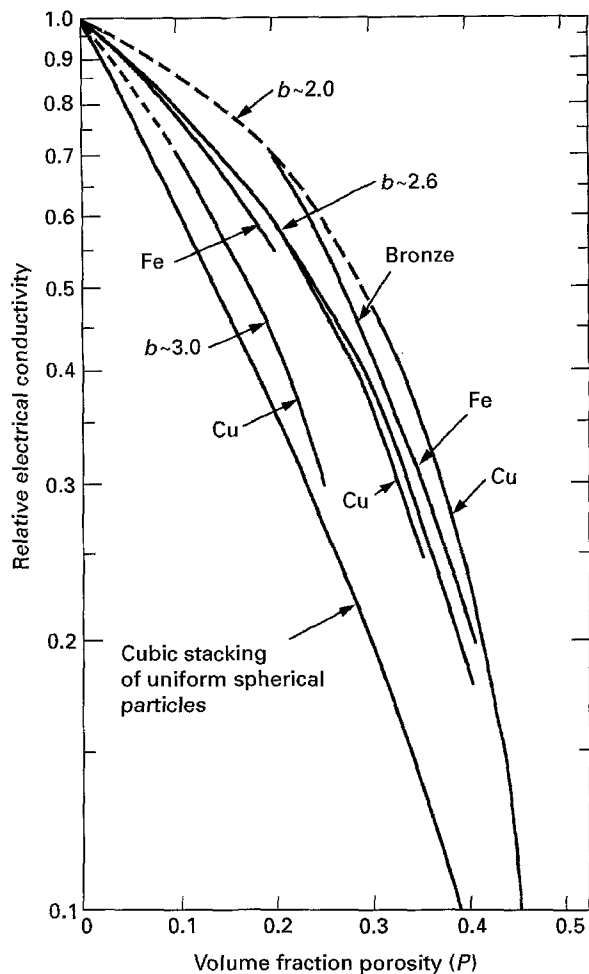
Figure 10 Relative electrical conductivity versus P (at 22 °C) for various metals. Note again the similarity in trend with that for Young's modulus, and tensile strength (Fig. 9) and hence again with cubic (thus approximately random) packing of spherical particles. Data from Jernot *et al.* [133].

strains are quite dependent on the nature of the stress [146], and other models show (v) either independent of, or decreasing with increasing, P generally consistent with data [14]. Two-dimensional computer models presented to support this increase, don't address how such a model (equivalent to assuming cylindrical pores) is pertinent to the assumed spherical porosity. Third, evaluation of these (and other models) has addressed the significant variations (shown in this study, even for the same material and similar processing, e.g. Figs 2,3,5, and 6) for different pore-processing combinations, e.g. tubular pores from extrusion versus denser particle packing from hot pressing. While not stated, data evaluated to support such models gave average b values of 3.6 ± 0.8 for E and 3.3 ± 1.1 for G, i.e. not reflecting broad evaluation of pore character.

Understanding effects of pore character on property-P dependance is important for practical, i.e. engineering purposes, i.e. to directly address processing-pore character relations. The models of Fig. 1 provide such guidance. Thus, since the fraction of solid is simply $1 - P$, design trade-offs between properties of interest and the weight of resultant parts are readily obtained. The development of ceramic sonar transducers with improved hydrostatic sensitivity was

guided by the models of Fig. 1 [147]. Thus, aligned, platelet pores (which behave similar to tubular pores) were seen as providing a much improved balance of hydrostatic sensitivity and mechanical integrity than pores between sintered particles (and not presenting sealing problems of either of the other two noted pore types).

Better understanding of property-P relations also requires broad understanding of specific variations in dependence of some properties, (as discussed further below) and of other processes [1]. Thus, refining models for the minimum solid area-P dependance for other material-process systems such as pores from leaching of phase separated, chemically derived (e.g. cement and plaster), and composite bodies (by various routes, e.g. chemical vapour infiltration (CVI) and with various pore-fibre-matrix relations) is important. However, such bodies are clearly expected to follow such models, as already shown for plaster [148] and CVI [149] bodies.

3.3. Evaluation and data quality

A basic question noted earlier is the quality of fitting of the models to the data, e.g. as measured by the standard deviation in the slope (b) value. While evaluation of the accuracy of model fitting is common and has been a focus of most of the previous studies, it has not played an explicit role in this evaluation for two reasons. First, quantitative evaluation of statistical fits was judged not to be necessary since data with a very limited P range or with substantial scatter was used only a limited amount, i.e. only in conjunction with other data. Second, and more fundamental, is the widely neglected fact that even data which is extensive and shows limited scatter is probably often of poorer quality than implied by the standard deviation or other measures of the "quality" of the data.

The basic data quality problem, especially for ceramics, that is almost universally neglected by investigators, is the issue of the homogeneity of the porosity. Lang *et al.* [125] were apparently the first to point this out. They noted that tests with different vibration modes (thus shifting the position of maximum stress in specimens) or different sized samples cut from the same piece of material typically resulted in consistent mechanical (e.g. elastic) property behaviour for well developed materials of high homogeneity (e.g. well-developed glasses and metals). However, they showed that normally such tests of ceramic materials gave differing results reflecting varying degrees of inhomogeneity. Subsequently, Spinner *et al.* [12] showed in their tests of ThO_2 as a function of porosity that they were not homogeneous. In fact they showed that variations generally increased with the amount of porosity as would be expected (Fig. 11). Similarly, Wu *et al.* [32] showed that differences in Young's modulus of B_4C at the upper limit of P (~15%) were as much as 13%, depending upon whether porosities of the actual bars measured, or the porosities of the original hot-pressed plates from which the bars were obtained, were used. Another important test of the homogeneity of the samples (or of the consistency of testing) is to
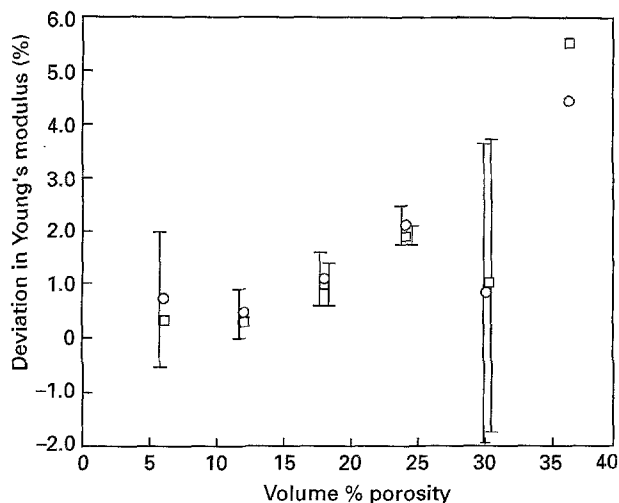
Figure 11 Deviations in Young's modulus versus P from Spinner et al.'s measurements of sintered ThO_2 samples tested in various vibration modes (at 22 °C) [12]. Their comparison was of vibrating bars edgewise versus flatwise (circles) and endwise (i.e. longitudinal) versus flatwise (squares) to determine Young's modulus. Since different modes stress different areas of the sample, this shows heterogeneity, which increases with P.

compare different directions of measurement (e.g. of elastic or conductivity properties) or comparison of inter-related (e.g. various elastic) properties [14]. Thus, comparison of Young's modulus with shear or bulk modulus or both is very useful. In particular, calculation of the Poisson's ratio and its dependence on porosity can be of considerable value, since it is a fairly sensitive indicator of differences, e.g. between E and G. Most models show no dependence of Poisson's ratio on porosity; some show Poisson's ratio decreasing with increasing porosity; none show it increasing with increasing porosity [14]. However, as noted earlier, while data of Chung et al. for MgO showed a substantial decrease of Poisson's ratio with increasing P, data of Spriggs et al. [42] and Soga and Anderson [13] showed a moderate increase in Poisson's ratio with P and data of Soga and Anderson [150] show a somewhat greater increase of Poisson's ratio with P. Thus, not only is there variability between the data sets, some trends are also inconsistent with theoretical expectations, which may reflect heterogeneity of the porosity. Although only about a quarter or less of the investigations of elastic properties allow calculation of Poisson's ratio as a function of porosity, there is still a considerable number that allow this as a possible indicator of heterogeneity. In view of these questions of the quality of much property–porosity data, it is both surprising and disappointing that use of polycrystalline values calculated from single crystal data is so limited (Figs 2–4, 8).

3.4 Mechanical property variations

All properties dependent on minimum solid area will be affected by porosity heterogeneities discussed above. Properties not changing the test specimen (or area) and reflecting spatial averages, e.g. elastic and conductive properties, will be affected less by such

heterogeneities. Mechanical properties that change the specimen or test area, for example by fracture, are potentially more susceptible to such variations, often in proportion to the scale and extent of change. However, hardness, and probably some wear tests, can be quite susceptible, e.g. due to indents being made less clear or of uncertain interpretation due to their interaction with heterogeneous porosity often being discarded as "bad" values.

There are also important variations that can occur due to crack–pore interactions that can be affected by heterogeneities in the porosity distribution, but are also probably intrinsic and depend on the scale of crack propogation, particularly of a single crack. Thus, particularly significant deviations can occur in fracture energy and toughness tests, where larger scale cracks have increased opportunity to develop crack bridging or branching via interaction with the pore structure that has little, or no, relation to effects on the scale of cracks controlling tensile strength [1, 151, 152].

In tensile testing, larger pores, or pore clusters, may affect, or in the extreme become, the failure initiating flaws, and hence affect strength [153–158], via the flaw size, geometry, and location, in addition to effects via fracture toughness K_{IC} (and hence via E and fracture energy γ) [150]. However, the cases where such effects are dominant are limited, mainly where there is extreme pore size (since most pores are small in comparison to the flaw sizes) [152]. The primary cases where pores are fracture origins are with isolated pores or pore clusters in relatively dense bodies often in association with heterogeneities of grain size, composition, or both [154,159]. When pores are the source of failure, they will change the strength–porosity trends significantly only when the resultant flaw size is significantly larger than other flaws that would have otherwise caused fracture. Further, in such cases, b values will be affected most by variations in the size of such large pores with P. Recently some strength–porosity variation due to porosity heterogeneity effects on machining flaws has been shown, [152] but mainly on highly elongated flaws.

Compressive strengths should also be affected by porosity heterogeneities, but such effects would appear to be more limited, since it is a cumulative damage process, thus typically involving many pores [160,161]. It has also been suggested as possibly having a higher porosity dependence due to its cumulative damage nature, hence possibly being affected by pore shape effects beyond those reflected in minimum solid area [14]. Similar possibilities were suggested for hardness [14]. However, the database for these suggestions is limited, and did not have the benefit of evaluating effects of processing–pore character of this study. The overall similarity of elastic–, strength–, hardness– and electrical or thermal conductivity–porosity dependencies shows that minimum solid area models are valid. This is also shown by the commonality of the porosity dependance for metals and ceramics since ductility in metals would limit their susceptibility to effects of porosity heterogeneities and pore shape and size effects, so greater metal–ceramic differences

TABLE VI Porosity dependence on dielectric constant

Material	Processing[a]	P[b] (%)	No. points[c]	B[d]	Investigator
SiO_2	S	3–85	> 18	0.84	Gannon et al. [162]
SiO_2	S	3–83	> 14	0.9	Harris and Welsh [50]
SiO_2	S	8–16	65	0.9	Harris and Welsh [50]
SiO_2	Foamed gel	50–80	6	0.8	Fujiu et al. [163]
Borosilicate glass	S	5–43	14	0.9	Sacks et al. [164]
TiO_2 (+ 14% ZrO_2)	S	5–38	13	1.5	Messer [165]
PZT	S	3–16	8	1.4	Biswai [166]
PZT	S	6–25	16	1.6	Hsueh et al. [167]
Si_3N_4	RS	22–32	4	1.2	Walton [168]

[a] S = Sintering, RS = reaction sintering.
[b] Volume fraction porosity (given as %).
[c] Number of data points (> indicates some data points reflected more than one measurement).
[d] Of Equation $E = E_0 (1 - BP)$, P = volume fraction (not %) porosity.

would occur if these dominated behaviour. However, as discussed elsewhere [1], the above issues are areas for possible refinement of the models. Such models are important because of their simplicity (especially for handling the real range of pore structures), and their applicability to a range of properties and materials over the whole range of achievable porosity.

3.5. Properties not following minimum solid area models
While minimum solid area models have broad applicability, as noted earlier, properties primarily, or exclusively, dependent on mass should instead follow a rule of mixture (and hence be independent of the character porosity) rather than minimum solid area relations. Of the possible properties dependent mainly on mass, e.g. heat capacity, refractive index ($n = K^{\frac{1}{2}}$), or dielectric constant ($K = n^2$), only a reasonable quantity of data was found for the latter. For this, the rule of mixtures gives

$$K = K_S (1 - P) + K_P P \qquad (2)$$

where K_S and K_P are the dielectric constants, respectively, of the solid and the pores. Since $P < 1$ (commonly < 0.5), and $K_P \sim 1$

$$K \sim K_S (1 - BP) \qquad (3)$$

a linear expression commonly used (where ideally $B = 1$). Note that plotting such a linear relation with $B = 1$ on a semi-log plot yields $b \sim 1$; thus, very low b values can be an indicator of a linear relation.

Literature data [50, 162–168] were found to fit Equation 3 reasonably well (as often shown by the investigators themselves). While there are deviations of B from 1, they are usually not large, and B averages ~ 1 (Table VI). Further, deviations of B below 1 are consistent with the fact that $K_P \sim 1$, not 0, which effectively reduces B. The high values of B are associated with higher K values, especially for TiO_2 and lead zirconate titanate (PZT), where charging effects within fine pores could be a factor. (This is supported by the fact that in Biswa's [166] PZT where part of the porosity was large spherical pores, which should exhibit less such charging effect, gave a somewhat lower

B value.) Variability of the B values again probably reflect porosity inhomogeneity, i.e. giving variable P levels in test samples cut from fabricated specimens, whose measured P values were assumed to be uniform.

4. Summary and conclusions
An extensive survey of the porosity dependence of the room temperature physical properties of materials shows that properties dependent on local flux or fields in the materials are consistent with minimum solid area models. Pertinent properties evaluated are elastic properties, tensile (flexure) and compressive strength, hardness, and electrical and thermal conductivities. Properties dependent on changes in the specimen or area tested, i.e. fracture and hardness may be more susceptible to effects of porosity heterogeneity and give broader variations. However, they still generally follow homogeneous minimum solid area models, unless there is extreme heterogeneity.

For properties following the minimum solid area models, overall consistency with the models is shown by the overall shape of the property–porosity curves. Thus, at lower P the log property versus P is an approximately straight line, which then gives way to a progressively more rapid property decrease with further increase in P, which is terminated by a precipitous property drop to zero at a critical P value (P_C). Typically, the linear trend occurs over approximately the first half of the $P = 0$ to P_C range. Data is consistent with lower linear slopes (b values) correlating with higher P_C values (e.g. > 0.5) associated with less dense particle packing and more open structures. Further, while low pressure extrusion gives low b values (e.g. ~ 2) consistent with expected elongated pores (e.g. from elongated areas of binder), die pressing and isopressing tend to progressively fall in between as expected, from their progressively intermediate particle packing, with colloidal processing and hot pressing giving higher b values consistent with denser particle packing.

Properties that should be determined more, or exclusively, by the volume fraction of solid mass fall above the minimum solid area models, as expected. Thus, dielectric constant was shown to follow the

commonly used linear relationship, an approximation of the expected rule of mixtures relationship.

Since completing this paper two studies of the flexure strength dependance of hot pressed NiO on porosity at 22 °C have been found reporting b values of 4.2 and 5.7, in good agreement with results in Table V [169, 170].

References

1. R. W. RICE, submitted for publication.
2. E. A. DEAN and J. A. LOPEZ, *J. Amer. Ceram. Soc.* **66** (1983) 366.
3. W. R. MANNING, O. HUNTER, Jr and B. R. POWELL, Jr, *Ibid.* **52** (1969) 436.
4. G. E. PORTU and P. VINCENZINI, *Ceramurgia Int'l,* **5** (1979) 165.
5. K. K. PHANI and S. K. NIYOGI, *J. Mater. Sci.* **22** (1987) 257.
6. D. R. PETRAK, D. T. RANKIN, R. RUH and R. D. SISSON, *J. Amer. Ceram. Soc.* **58** (1975) 78.
7. K. K. PHANI, *J. Mater. Sci. Lett.* **51** (1986) 747.
8. J. BOOCOCK, A. S. FURZER and J. R. MATTHEWS, Report: AERE-M2565, Process Technology Division, Atomic Energy Research Establishment, Harwell, Berkshire, England (1972).
9. K. K. PHANI and S. K. NIYOGI, *J. Mater. Sci. Lett.* **5** (1986) 427.
10. S. K. DATTA, A. K. MUKHOPADHYAY and D. CHAKRABORTY, *Amer. Ceram. Soc. Bull.* **48** (1989) 2098.
11. A. SALAK, V. MISKOVIC, E. DUDROVA and E. RUDNAYOVA, *Pwd. Met. Mater.* **6** (1974) 128.
12. S. SPINNER, F. P. KNUDSEN and L. STONE, *J. Research, National Bureau of Standards,* **67C** (Jan–Mar 1963) 39.
13. N. SOGA and E. SCHREIBER, *J. Amer. Ceram. Soc.* **51** (1968) 465.
14. R. W. RICE, in "Treatise on materials science and technology, Vol. II, properties and microstructure," edited by R. K. McCrone (Academic Press, Inc., New York, 1977) p.199.
15. K. K. SCHILLER, in "Mechanical properties of non-metallic brittle materials," edited by W. H. Walton, (Interscience Publishers, Inc., 1958) p.35.
16. K. P. KNUDSEN, *J. Amer. Ceram. Soc.* **48** (1959) 376.
17. R. W. RICE and S. W. FREIMAN, in "Ceramic microstructures, 76," edited by R. M. Fulrath and J. A. Pask (Westview Press, Boulder, CO, 1977) p.800.
18. B. PAUL, *Trans. Metal. Soc. AIME,* **218** (1960) 36.
19. M. EUDIER, *Powder Metall.* **9** (1962) 278.
20. O. ISHAI and L. J. COHEN, *Int. J. Mech. Sci.* **9** (1967) 539.
21. R. W. RICE, *J. Amer. Ceram. Soc.* **59** (1976) 536.
22. J. H. ENLOE, R. W. RICE, J. W. LAU, R. KUMAR and S. Y. LEE, *J. Amer. Ceram. Soc.* **74** (1991) 2214.
23. J. S. O'NEILL, *Trans. Brit. Ceram. Soc.* **69** (1970) 82.
24. H. TOMASZEWSKI, *Ceram. Int.* **8** (1982) 60.
25. J. C. KNIGHT and T. F. PAGE, *Brit. Ceram. Trans. J.* **85** (1986) 27.
26. R. L. COBLE and W. D. KINGERY, *J. Amer. Ceram. Soc.* **39** (1956) 377.
27. J. C. WANG, *J. Mater. Sci.* **19** (1984) 809.
28. L. SZTANKOVICS, *Epitoanyag* **42** (1990) 88.
29. H. NEUBER and A. WIMMER, Technical Report AFML-TR-68-23, Air Force Materials Laboratory, Wright-Patterson Air Force Base, OH (March 1968).
30. D. B. BINNS and P. POPPER, *Proc. Brit. Ceram. Soc.* **6** (1966) 71.
31. D. J. GREEN, C. NADER and R. BREZNY, in "Sintering of advanced ceramics", edited by C. A. Handwerker, J. E. Blendell and W. Kaysser, (*American Ceramics Society*, Westerville, OH, 1990). p.347.
32. C. C. WU and R. W. RICE, *Ceram. Eng. and Sci. Proc.* **6** (1985) 977.
33. D. R. PETRAK, R. RUH and G. R. ATKINS, *Bull. Amer. Ceram. Soc.* **53** (1974) 569.
34. B. A. CHANDLER, E. C. DUDERSTADT and J. F. WHITE, *J. Nucl. Mater.* **8** (1963) 329.
35. R. E. FRYXELL and B. A. CHANDLER, *J. Amer. Ceram. Soc.* **47** (1964) 283.
36. J. S. O'NEILL and D. T. LIVEY, United Kingdom Atomic Energy Authority Research Report # AERER 4912 (1965).
37. A. ARGOITIA, J. F. BAUMARD and C. GAULT, in "High tech ceramics", edited by P. Vincenzini (Elsevier Science Publishers B. V., Amsterdam, The Netherlands, 1987). p.1381.
38. S. L. DOLE, O. HUNTER, Jr and F. W. CALDERWOOD, *J. Amer. Ceram. Soc.* **63** (1980) 136.
39. S. L. DOLE and O. HUNTER, Jr, *Comm. Amer. Ceram. Soc.* March (1983) C47.
40. O. HUNTER, Jr, R. W. SCHEIDECKER and S. TOJO, *Ceramurgia Int.* **5** (1979) 137.
41. S. L. DOLE, O. HUNTER, Jr, and C. J. WOOGE, *J. Amer. Ceram. Soc.,* **60** (11–12) (1977) 488.
42. R. M. SPRIGGS, L. A. BRISSETTE and T. VASILOS, *Ibid.* **45** (1962) 400.
43. K. R. JANOWSKI and R. C. ROSSI, *Ibid.* **51** (1968) 453.
44. R. B. BIDDULPH, M.Sc. Thesis, Department of Ceramic Engineering, University of Utah (June 1964).
45. W. R. MANNING, Ph.D. Thesis, Ames Laboratory, USAEC. Iowa State University (June 1972).
46. J. A. HAGLUND and O. HUNTER, Jr, *J. Amer. Ceram. Soc.* **56** (1973) 327.
47. O. HUNTER, Jr and G. E. GRADDY, Jr, *J. Amer. Ceram. Soc.* **59** (1976) 82.
48. O. HUNTER, Jr, H. J. KORKLAN and R. R. SUCHOMEL, *Ibid.* **57** (1974) 267.
49. S. L. DOLE, O. HUNTER, Jr and F. W. CALDERWOOD, *Ibid.* **60** (1977) 167.
50. J. N. HARRIS and E. A. WELSH, NSC Special Publication (May, 1973).
51. G. M. TOMILOV, Translated from Izvestiya Akademii Nauk SSSR, *Neorganicheskie Materialy,* **13** (1977) 117.
52. S. C. PARK and L. L. HENCH in "Physical properties of partially densified SiO_2 gels," edited by L. L. Hench and D. R. Ulrich (Wiley-Interscience Publication, New York, 1986).
53. C. E. CURTIS and J. R. JOHNSON, *J. Amer. Ceram. Soc.* **40** (1957) 63.
54. J. P. PANAKKAL and J. K. GHOSH, *J. Mater. Sci. Lett.* **3** (1984) 835.
55. M. O. MARLOWE and D. R. WILDER, *J. Amer. Ceram. Soc.* **48** (1965) 227.
56. C. F. SMITH and W. B. CRANDALL, *Ibid.* **47** (1964) 624.
57. P. A. EVANS, R. STEVENS and S. R. TAN, *Brit. Ceram. Trans. J.* **83** (1984) 43.
58. C. CHU, K. BAR, J. P. SINGH, K. C. LORETTA, M. C. GILLONE, R. P. POEPPEL and J. L. ROUTFORT, *J. Amer. Ceram. Soc.* **72** (1989) 1643.
59. E. SCHREIBER, *Ibid.* **51** (1968) 541.
60. D. F. PORTER, J. S. REED and DAVID LEWIS III, *Ibid.* **60** (1977) 347.
61. R. A. PENTY, D. P. H. FLASSELMAN and R. M. SPRIGGS, *Ibid.* **55** (1971) 169.
62. B. L. METCALFE and J. H. SANT, *Brit. Ceram. Soc.* **74** (1975) 193.
63. D. WILLS and J. MASIULANIS, *J. Can. Ceram. Soc.* **45** (1976) 15.
64. N. McALFORD, J. D. BIRCHALL, W. J. CLEGG, M. A. HARMER, K. KENDALL and D. H. JONES, *J. Mater. Sci.* **23** (1988) 761.
65. B. BRIDGE and R. ROUND, *Ibid.* **8** (1989) 691.
66. N. CLAUSSEN, *Mater. Sci. Eng.* **4** (1969) 243.
67. A. G. KING and W. M. WHEILDON, Paper presented at Eleventh Meeting of the Refractory Composites Working Group, Los Angeles, CA, January 25–27, 1986.
68. V. MANDORF and J. HARTWIG, in "High temperature materials" Vol. 11 edited by G. M. Ault, W. F. Barclay and H. P. Munger, (Interscience Publishers, New York, 1963). p. 455.
69. J. R. COST, K. R. JANOWSKI and R. C. ROSSI, Aerospace Corp. Air Force Report # SAMSO-TR-68-28 (January 1968).
70. R. S. LIEBLING, *Mater. Res. Bull.* **2** (1967) 1035.

71. B. CHAMPAGNE and R. ANGERS, *J. Amer. Ceram. Soc.* **62** (1979) 149.
72. M. BEAUVY, *Rev. Int. Hautes Templer. Refract. Fr.* **19** (1982) 301.
73. K. A. SCHWETZ, W. GRELLNER and A. LIPP *Inst. Phys. Con L. Ser.* **75** (1986) 413.
74. G. W. HOLLENBERG and G. WALTHER, *J. Amer. Ceram. Soc.* **11–12** (1980) 610.
75. A. D. OSIPOV, I. T. OSTAPENKO, V. V. SLEZOV, R. V. TARASOV, V. P. PODTYKAN, and N. F. KARTSEV, Kharkov Physicotechnical Institute, Academy of Sciences of the Ukrainian SSR; Translated from *Poroshkovaya Metallurgiya*, **1** (1982) p. 63.
76. F. P. KNUDSEN, *J. Amer. Ceram. Soc.* **42** (1959) 376.
77. T. D. GULDEN, *Ibid.* **52** (1969) 585.
78. W. S. COBLENZ, *Ibid.* **58** (1975) 530.
79. D. BROUSSAUD, J. P. DUMAS and Y. LAZENNEC, in "Ceramic microstructures'76", (edited by R. M. Fulrath and J. A. Pask (Westview, Press, Boulder, Colorado, 1977) p. 679.
80. R. D. CARNAHAN, *J. Amer. Ceram. Soc.* **51** (1968) 223.
81. S. PROCHAZKA, C. A. JOHNSON, and R. A. GIDDINGS, Final Report for Contract N62269-75-C-0122.
82. S. G. SESHADRI, M. SRINIVASAN and K. Y. CHIA, Ceramic Trans. 2, Silicon Carbide, (*Amer. Ceram. Soc*, 1989) 215–255.
83. O. CROIX, M. GOUNOT, P. BERGEZ, M. LUCE and M. CAUCHETIER, in "Ceramics today–tomorrow's ceramics" Vol. 66B edited by P. Vincenzini (Elsevier Science Publishers B. V., Amsterdam, The Netherlands p. 1447.
84. V. P. BULYCHEV, R. A. ANDRIEVSKII, and L. B. NEZHEVENKO, "Poroshkovaya Metalurgia" Vol 4 (Plenum Publishing, New York, 1977) p. 273.
85. P. BOCH, J. C. GLANDUS, J. JARRIGE, J. P. LECOMPTE and J. MEXMAIN, *Ceram. Int.* **8** (1982) 34.
86. A. S. BUBNOV, V. P. ZLOBIN, D. F. KARLOV. V. A. BARSUK. V. M. NESTERENKO, V. YA. PETROVSKII and E. I. GERVITS, *Poroshkovaya Metallurgiya*, **8** (1986) 89.
87. W. A. FATE, *J. Amer. Ceram. Soc.* **57** (1974) 372.
88. O. YEHESKEL and Y. GEFEN, *Mat. Sci. Eng.* **71** (1985) 95.
89. G. DePORTU and P. VINCENZINI, *Ceramurgia Int.* **6** (1980) 129.
90. D. C. LARSEN, J. W. ADAMS, L. R. JOHNSON, A. P. S. TEOTIA and L. G. HILL, "Ceramic materials for advanced heat engines" (Noyes Publication, Park Ridge, NJ, 1985).
91. R. W. RICE, *J. Mater. Sci.* **12** (1977) 627.
92. M. DESMAISON-BRUT, J. C. GLANDERS, J. MONTINTIN, F. VALIN and M. BONCOEUR, in "Ceramics today–tomorrow's ceramics," Vol. 66C, edited by P. Vincenzini (Elsevier Science Publishers B. V., Amsterdam, 1991). p. 1713.
93. P. BOCH and J. C. GLANDUS, *J. Mater. Sci.* **14** (1979) 379.
94. M. C. UDY and F. W. BOULGER, "Variation of modulus of elasticity of beryllia with density. The properties of beryllium oxide, BMI-T-18" (Batelle Memorial Inst., Columbus, OH, 1949).
95. J. ELSTON and C. LABBE, *J. Nucl. Mater.* **4** (1961) 143.
96. R. L. HELFERICH and C. A. ZANIS, NSR Special Publication, Report 3911, Bethesda, MD (1973).
97. S. CHO, F. J. ARENAS and J. OCHOA, *Ceram. Int.* **16** (1990) 301.
98. P. P. BUDNIKOV, F. KERBE and F. J. CHARITONOV, "Science of ceramics," Vol 4 edited by G. H. Stewart, (The British Ceramic Society, London, 1968) p. 69.
99. K. OKAZAKI and K. NAGATA, in Proceedings 1971 International Conference on Mechanical Behavior of Materials IV (*Soc. Mat. Sci*, Kyoto, Japan, 1972) p. 404.
100. V. M. GROPYANOV, V. L. KUZNETSOVA and L. K. KLIMOVA, Translated from *Poroshkovaya Metallurgia* **8** (Plenum Publishing, New York, NY, 1977) p. 609.
101. E. E. HUCKE, University of Michigan Report for Advanced Research Projects Agency Order No. 1824 (1972).
102. O. YAMADA, Y. MIYAMOTO and M. KOIZUMI, *J. Amer. Ceram. Soc.* **7–0** (1987) C206.
103. A. K. MUKHOPADHYAY, S. K. DATTA and D. CHAKRABORTY, *Ceram. Int.* **17** (1991) 121.
104. W. J. GARDNER, J. D. McCLELLAND and J. H. RICHARDSON, Aerospace Corp. Report # TDR-269 (4240-01)-1 for A. F. Contract # 04(695)-269, September (1963).
105. J. E. HOVE and W. C. RILEY (editors), "Introduction: Ceramics for advanced technologies" (John Wiley & Sons, Inc., New York, 1965). p. 5.
106. P. MURRAY, Aerospace Corp. Report # TDR-269(4240-01)-1 for A. F. Contract # 04(695)-269, September (1963).
107. National Beryllia Corporation Brochure "Designing With Beryllia," (1976).
108. E. RYSHKEWITCH and D. W. RICHERSON, "Oxide ceramics" (Academic Press, Inc., Orlando, FL, (1985) p. 237.
109. R. W. POWELL, *Trans. Brit. Ceram. Soc.* **53** (1954) 389.
110. I. C. HOBSON, R. TAYLOR and J. B. AINSCOUGH, *J. Phys. D: A2121, Phys.* **7** (1974) 1003.
111. J. C. VAN CRAEYNEST and J. P. STORA, *J. Nucl. Mater.* **37** (1970) 153.
112. J. P. MOORE and D. L. MCELROY, *J. Amer. Ceram. Soc.* **54** (1971) 40.
113. A. M. ROSS, "The dependence of the thermal conductivity of uranium dioxide on density, microstructure, stoichiometry and thermal-neutron irradiation" (Atomic Energy of Canada Limited, Chalk River, Ontario, 1960).
114. T. SAEGUSA, K. KAMATA, Y. LIDA and N. WAKAO, *Kagaku Kogaku* **37** (1973) 811; translated by Y. Lida, Yokohama National University, Minami-ku, Yokohama.
115. A. SUGAWARA and Y. YOSHIZAWA, *J. AV121. Phys.* **33** (1962) 3135.
116. P. WAGNER, J. A. O'ROURKE, and P. E. ARMSTRONG, *J. Amer. Ceram. Soc.* **55** (1972) 214.
117. S. K. RHEE, *J. Mat. Sci. Eng.* **20** (1975) 89.
118. S. K. RHEE, *J. Amer. Ceram. Soc.* **55** (1972) 580.
119. D. S. RUTMAN, A. F. MAURIN, G. A. TAKSIS, and Y. S. TOROPOV, *Refractories* **5–6** (1970) 371.
120. G. V. SAMSONOV and V. E. MATSERA, *Sov. Powd. Met. Mater. Ceram.* **11** (1972) 719.
121. V. P. BULYCHEV, R. A. ANDRIEVSKII, and L. B. NEZHEVENKO, Translated from *Poroshkovaya Metallurgiya* **4** (1977) 38.
122. E. A. BELSKAYA and A. S. TARABANOV, Translated from *Inzhenerno-Fizicheskii Zhurnal*, **20** (1971) 654.
123. F. P. KNUDSEN, *J. Amer. Ceram. Soc.* **45** (1962) 94.
124. D. H. CHUNG and W. R. BUESSEM, in Proceedings International Symposium 6, edited by F. W. Vahldiek and S. A. Mersol (Plenum Press, NY, 1968) p. 217.
125. S. M. LANG, National Bureau of Standards Monograph 6, US Government Printing Office, Washington, DC (1960).
126. J. B. WACHTMAN, Jr. and D. G. LAM, Jr, *J. Amer. Ceram. Soc.* **42** (1959) 254.
127. D. H. CHUNG, P. O. BENSON and W. B. CRANDALL, Progress Report 6, Contract DA-31-124-ARO (D-23), Army Research Office, Durham, NC (1963).
128. G. R. TERWILLIGER, BS Thesis, State University of New York, College of Ceramics, Alfred, New York (1964).
129. J. T. BAILEY and R. RUSSELL, Jr, *Brit. Ceram. Soc.* **68** (1969) 169.
130. D. M. CHAY, H. PALMOUR III, and W. W. KRIEGEL, *J. Amer. Ceram. Soc.* **51** (1968) 10.
131. P. D. WILCOX and I. B. CUTLER, *Ibid.* **49** (1966) 249.
132. J. P. PANAKKAL and J. K. GHOSH, *J. Mater. Sci. Lett.* **3** (1984) 935.
133. J. P. JERNOT, M. COSTER and J. L. CHERMANT, *Powder Technol.* **30** (1981) 21.
134. G. D. MCADAM, *J. Iron and Steel Institute* August (1951) 346.
135. D. POHL, *Powd. Metall. Int.* **1** (1969) 26.
136. K. K. PHANI and R. N. MURKERJEE, *J. Mater. Sci.* **22** (1987) 3453.
137. G. LEWIS, *J. Can. Ceram. Soc.* **62** (1993) 258.
138. J. P. SINGH, H. J. LEU, R. B. POEPPEL, E. VAN VOORHEES, G. T. GOUDEY, K. WINSLEY, and DONGLU SHI, *J. Appl. Phys.* **66** (1989) 3154.
139. H. M. LEDBETTER, M. W. AUSTIN, S. A. KIM, and MING LEI, *J. Mater. Res.* **2** (1987) 786.

140. H. LEDBETTER, Ibid. **7** (1992) 2905.
141. H. LEDBETTER and MING LEI, Ibid. **6** (1991) 2253.
142. R. ROUND and B. BRIDGE, J. Mater. Sci. Lett. **6** (1987) 1471.
143. R. M. CHRISTENSEN, J. Mech. Phys. Solids **38** (1990) 379.
144. N. RAMAKRISHNAN and V. S. ARUNACHALAM, J. Amer. Ceram. Soc. **76** (1993) 2745.
145. R. W. RICE, J. Mater. Sci. **28** (1993) 2187.
146. Idem. submitted for publication.
147. R. W. RICE, M. KAHN, and D. E. SHADWELL, US Patent 4683, 161&/28/87.
148. I. SOROKA and P. J. SEREDA, J. Amer. Ceram. Soc. **51** (1968) 337.
149. R . W. RICE and D. LEWIS III, "Reference Book of Composites Technology, VI" edited by S. M. Lee (Technomic Pub., Lancaster, PA 1989) p. 117.
150. N. SOGA and O. L. ANDERSON, J. Amer. Ceram. Soc. **49** (1966) 318.
151. R. W. RICE, submitted to J. Mater. Sci.
152. Idem., submitted to J. Mater. Sci.
153. A. G. EVANS and G. TAPPIN, Proc. Brit. Ceram. Soc. **20** (1972) 275.
154. R. W. RICE, J. Mater. Sci. **19** (1984) 895.
155. Idem., "Processing of crystalline ceramics", edited by H. Palmour, R. Davis and T. Hare (Plenum Press, New York, NY, 1978) p. 303.
156. Idem., Special Technical Publication 827 (ASTM, Philadelphia, PA, 1984).
157. Idem., Mater. Sci. Eng. **A112** (1989) 215.
158. R. W. RICE, J. J. MECHOLSKY, S. W. FREIMAN and S. M. MOREY, NRL Memo Report 4075 (1979).
159. R. W. RICE, in press.
160. Idem., in "Ceramics in severe environments", edited by W. Kriegel (Plenum Press, New York, 1971) p. 195.
161. J. LANKFORD, J. Hard Mater. **2** (1991) 55.
162. R. E. GANNON, G. M. HARRIS and T. VASILOS, Amer. Ceram. Soc. Bull. **44** (1965) 460.
163. T. FUJIU, G. L. MESSING and W. HUEBNER, Ibid. **73** (1990) 85.
164. M. D. SACKS, M. S. RANDALL, G. W. SCHEIFFELE, R. RAGHUNATHAN and J. H. SIMMONS, Ceram. Trans. (American Ceramics Society, Westerville, OH, 1991) p. 407.
165. P. F. MESSER, T. & J. Brit. Ceram. Soc. **82** (1983) 190.
166. D. R. BISWAS, J. Amer. Ceram. Soc. (1978) 461.
167. C.-C. HSUEU, M. L. MECARTNEY, W. B. HARRISON, M. R. B. HANSON and B. G. KOEPKE, J. Mater. Sci. Lett. **8** (1989) 1209.
168. J. D. WALTON, Jr, Ceram. Bull. **53** (1974) 255.
169. R. M. SPRIGGS, L. A. BRISSETTE and T. VASILIOS, Amer. Ceram. Bull. **43** (1964) 572.
170. W. B. HARRISON, Third Technical Report for ARO Contract No. DA-11-022-ORD-3441, March (1965).